The 2012 World Congress on
Advances in Civil, Environmental, and Materials Research (ACEM' 12)
Seoul, Korea, August 26-30, 2012

Modification of Flutter Derivatives Satisfying the Causality Condition for the Time-domain Aeroelastic Analysis

*Kilje Jung[1)] Ho-Kyung Kim[2)] and Hae Sung Lee[3)]

[1), 2), 3)] *Department of Civil and Environmental Engineering, Seoul National University, Seoul, Korea*
[1)] *kjjung01@snu.ac.kr*

ABSTRACT

The difficulty in aeroelastic analysis basically arises from the frequency dependence of the aeroelastic forces. Therefore, the frequency dependence should be eliminated for the time-domain analysis of the aeroelastic system by applying the convolution integral approach. However, the convolution integral is valid if the impulse response function vanishes for $t<0$, which is referred to as the causality condition. Although the RFA is the most well-known approach to adjust the flutter derivatives for satisfying the causality condition, the RFA shows the limitation in application of the bluff section. In this study, a new modification method is presented by optimization with penalty function and the proposed method is verified via two numerical examples of thin rectangular section and bluff H-type section.

1. INTRODUCTION

The difficulty in aeroelastic analysis basically arises from the frequency dependence of self-excited forces. Although they are given in the time domain, the self-excited forces proposed by Scanlan and Tomko are essentially based on transfer functions between deck motions and the self-excited forces in the frequency domain. Therefore, an aeroelastic analysis in the frequency domain (Katsuchi 1999) is more widely employed than one in the time domain (Chen 2000). However, the importance of time-domain analysis has been increasingly recognized for investigating structural nonlinearities and transient responses caused by non-stationary wind (Chen 2003). The difficulty of the time-domain aeroelastic analysis arises from the frequency dependence of the self-excited forces defined by flutter derivatives. Without the elimination of the frequency dependence, a frequency-domain analysis should be performed for a time-domain

[1)] Postdoctoral Res. Assoc.
[2)] Associate Professor
[3)] Professor

analysis to obtain frequency information on deck motion. To circumvent this complexity, the rational function approximation (RFA), which expresses aerodynamic forces by the convolution of deck motion using impulse response functions, has been widely adopted (Chen 2000). Since, however, the RFA is the extension of the method that has been used in the aeronautical field for the application to a wing of an airplane, there is a certain limitation to apply the RFA for the bluff sections frequently selected in bridge design (Caracoglia 2003). This study presents a new approach for evaluating impulse response functions for the convolution integrals of aerodynamic forces using optimization in the frequency domain.

2. EVALUATION OF AERODYNAMIC FORCES

A section model with two degrees of freedom in vertical (h) and rotational (α) direction is subjected to self-excited forces in the direction of each DOF. Then, the equation of motion per unit length is expressed as follows:

$$\begin{aligned} m_h\ddot{h} + c_h\dot{h} + k_h h &= L_{ae}(t) + L_{ex}(t) \\ m_\alpha\ddot{\alpha} + c_\alpha\dot{\alpha} + k_\alpha\alpha &= M_{ae}(t) + M_{ex}(t) \end{aligned} \tag{1}$$

where m_i, c_i and k_i are the mass, damping and stiffness in the direction of i=h, α, respectively, while L_{ae}, M_{ae}, L_{ex}, M_{ex} are the self-excited lift force, moment and external excitation forces in the h and α direction, respectively. The overhead dot denotes differentiation with respect to time.

In accordance with the Scanlan and Tomko's formulation(Scanlan 1971), the self-excited forces acting on a sinusoidally oscillating section in a single frequency are defined as:

$$\begin{aligned} L_{ae} &= \frac{1}{2}\rho U^2 B[KH_1^*\frac{\dot{h}}{U} + KH_2^*\frac{B\dot{\alpha}}{U} + K^2H_3^*\alpha + K^2H_4^*\frac{h}{B}] \\ M_{ae} &= \frac{1}{2}\rho U^2 B^2[KA_1^*\frac{B\dot{h}}{U} + KA_2^*\frac{B\dot{\alpha}}{U} + K^2A_3^*\alpha + K^2A_4^*\frac{h}{B}] \end{aligned} \tag{2}$$

where ρ is the air density, U is the mean wind velocity, B is the width of the section model. K=$B\omega/U$ is the reduced frequency where ω is the angular frequency of the oscillation. The flutter derivatives are denoted as H_m^* and A_m^* (m=1,2,3,4), and are functions of the angular frequency.

The general solution of Eq. (1) consists of the homogeneous and particular solution. In case the aerodynamic forces are defined as Eq. (2) proposed by Scanlan and Tomko, the particular solution of Eq. (1) is easily determined for given external harmonic excitation forces. However, it is difficult to obtain the homogeneous solution of Eq. (1) because the aerodynamic forces of Eq. (2) are dependent on unknown modal frequencies and shapes of the 2-DOF system. To circumvent this computational complexity, the aerodynamic forces are usually defined in the frequency domain as follows:

$$\begin{pmatrix} F(L_{ad}) \\ F(M_{ad}) \end{pmatrix} = \frac{1}{2}\rho U^2 \begin{bmatrix} iK^2H_1^* + K^2H_4^* & B(iK^2H_2^* + K^2H_3^*) \\ B(iK^2A_1^* + K^2A_4^*) & B^2(iK^2A_2^* + K^2A_3^*) \end{bmatrix} \begin{pmatrix} F(h) \\ F(\alpha) \end{pmatrix}$$
$$= \begin{bmatrix} i\phi_{hh}^I + \phi_{hh}^R & i\phi_{h\alpha}^I + \phi_{h\alpha}^R \\ i\phi_{\alpha h}^I + \phi_{\alpha h}^R & i\phi_{\alpha\alpha}^I + \phi_{\alpha\alpha}^R \end{bmatrix} \begin{pmatrix} F(h) \\ F(\alpha) \end{pmatrix} = \begin{bmatrix} F(\Phi_{hh}) & F(\Phi_{h\alpha}) \\ F(\Phi_{\alpha h}) & F(\Phi_{\alpha\alpha}) \end{bmatrix} F(\mathbf{u}) \tag{3}$$

where *F* denotes the Fourier transform, and *i* is the imaginary unit. ϕ_{mn}^I and ϕ_{mn}^R are the imaginary and real part of transfer function, respectively. Φ_{mn} is the impulse response function representing the aerodynamic force in the *m* direction at time *t* induced by the unit impulse motion of a section in the *n* direction at $t = 0$. Since no aerodynamic force is generated before the section moves, the causality condition should be satisfied, that is, the impulse response function vanishes for $t < 0$ (Jung 2012). As the flutter derivatives are given, the impulse response function is readily obtained by the inverse Fourier transform of the transfer function:

$$\Phi_{mn}(t) = \frac{1}{2\pi}\int_{-\infty}^{\infty}(i\phi_{mn}^I + \phi_{mn}^R)e^{i\omega t}d\omega \tag{4}$$

Since the impulse response functions should be real-valued functions, the causality condition of the impulse response function is expressed as follows:

$$\int_0^{\infty}(\phi_{mn}^R(\omega)\cos\omega t - \phi_{mn}^I(\omega)\sin\omega t)d\omega = 0 \text{ for } t < 0 \tag{5}$$

Utilizing the convolution theorem of the Fourier transform, the aerodynamic forces in the time domain are evaluated by the following convolution integrals:

$$L_{ae}(t) = \frac{1}{2}\rho U^2 B(\int_0^t \Phi_{hh}(t-\tau)\frac{h(\tau)}{B}d\tau + \int_0^t \Phi_{h\alpha}(t-\tau)\alpha(\tau)d\tau)$$
$$M_{ae}(t) = \frac{1}{2}\rho U^2 B^2(\int_0^t \Phi_{\alpha h}(t-\tau)\frac{h(\tau)}{B}d\tau + \int_0^t \Phi_{\alpha\alpha}(t-\tau)\alpha(\tau)d\tau) \tag{6}$$

The flutter derivatives are extracted at several discrete frequencies, and thus the transfer functions are defined discretely as well at the extraction frequencies rather than in a continuous fashion. To perform the integration in Eqs. (4) and (5), each part of the transfer function between two adjacent extraction frequencies is interpolated. The interpolation function for the transfer function plays the same role as a finite element in the finite element method, and should be selected to approximate real transfer functions accurately with the finite number of the extraction frequencies. Cubic spline, which is a piecewise 3rd-order polynomial (Kreyszig 1999), is selected to form a smooth and continuous function without derivative information.

3. EVALUATION OF IMPULSE RESPONSE FUNCTIONS BY OPTIMIZATION

The measured transfer functions should be modified so as to vanish identically in the negative time domain. This modification procedure is defined as an optimization problem for finding a transfer function closest to the measured transfer function subject to the causality constraint.

$$
\begin{aligned}
&\underset{\theta^R_{mn},\theta^I_{mn}}{\mathrm{Min}}\ \Pi_{mn}(\theta^R_{mn},\theta^I_{mn}) = \frac{1}{2}\frac{w_{mn}}{\left\|\phi^R_{mn}\right\|^2_{L_2}}\int_0^{\omega_{\max}}(\theta^R_{mn}-\phi^R_{mn})^2\,d\omega + \frac{1}{2}\frac{(1-w_{mn})}{\left\|\phi^I_{mn}\right\|^2_{L_2}}\int_0^{\omega_{\max}}(\theta^I_{mn}-\phi^I_{mn})^2\,d\omega \\
&\qquad \text{subject to } \int_0^{\omega_{\max}}(\overline{\theta}^R_{mn}\cos\omega t-\overline{\theta}^I_{mn}\sin\omega t)\,d\omega = 0 \ \text{ for } t<0
\end{aligned}
\tag{7}
$$

where θ^R_{mn} and θ^I_{mn} denote the real and the imaginary part of the modified transfer function, respectively, and w_{mn} is a prescribed weighting factor ranging from 0 to 1, which adjusts the relative weight between the real and imaginary part of the transfer function in the optimization. The normalization of each term in the object function is applied to level the magnitude of each term. The L_2 norm of a function is denoted as $\left\|\cdot\right\|_{L_2}$ in Eq. (7).

Since the causality condition contains an independent variable, i.e., time *t*, it is difficult to enforce the constraint in a strong sense. Rather, in this study, the causality condition is imposed in a weak sense using the penalty function approach.

$$
\begin{aligned}
&\underset{\theta^R_{mn},\theta^I_{mn}}{\mathrm{Min}}\ \Pi_{mn}(\theta^R_{mn},\theta^I_{mn}) = \frac{1}{2}\frac{w_{mn}}{\left\|\phi^R_{mn}\right\|^2_{L_2}}\int_0^{\omega_{\max}}(\theta^R_{mn}-\phi^R_{mn})^2\,d\omega + \frac{1}{2}\frac{(1-w_{mn})}{\left\|\phi^I_{mn}\right\|^2_{L_2}}\int_0^{\omega_{\max}}(\theta^I_{mn}-\phi^I_{mn})^2\,d\omega + \\
&\qquad \frac{\lambda^2_{mn}}{2}\int_{-T_{\max}}^{0}\left(\int_0^{\omega_{\max}}(\overline{\theta}^R_{mn}\cos\omega t-\overline{\theta}^I_{mn}\sin\omega t)\,d\omega\right)^2 dt
\end{aligned}
\tag{8}
$$

Here, λ_{mn} and $T_{\max}$ are the penalty number and the maximum time duration for the time integration of the penalty term, respectively. The time duration for the time integration of the penalty function is assumed to be the same as the maximum time used in the time-domain analysis of Eq. (1). The equal weighting of $w_{mn} = 0.5$ yields balanced results for all cases examined in this study. The weighting factor may be adjusted for a balanced solution, if necessary.

The penalty number controls the strength of the causality condition imposed in the optimization. As the penalty number becomes smaller, the effect of the causality condition on the solution of the optimization problem of Eq. (8) becomes weaker, and the solution converges to the measured transfer function. The one-sided convolution integrals for the aerodynamic forces lose mathematical robustness for a small penalty number due to the violation of the causality condition. On the other hand, the causality condition has a dominant influence on the optimization for a large penalty number, and the solution deviates from the measured transfer function, which causes Eq. (1) to yield solutions inconsistent with measured responses. Therefore, it is very crucial to determine a well-balanced penalty number for obtaining an accurate and mathematically meaningful solution of Eq. (1) in the time-domain aeroelastic analysis.

A series of extensive numerical tests conducted in this study revealed that the penalty number that reduces the penalty function to 2% of its original value before the optimization yields well-balanced solutions, and that the order of magnitude of the optimal penalty number usually is about 10^{-1}. Since a solution obtained in the penalty function formulation does not sensitively vary with the penalty number, a penalty number of 0.1 may be selected without further calculations. For more precise solutions, however, the optimization problem of Eq. (8) has to be solved for several different penalty numbers to find the penalty number satisfying the aforementioned criterion.

4. NUMERICAL EXAMPLE OF THE SECTION MODEL

The validity of the proposed method is demonstrated through the example on a bluff H-type section. The transfer functions and the corresponding impulse response functions evaluated by the proposed method and RFA are presented. The flutter derivatives are extracted from forced vibration tests in wind tunnel. The experiment for a bluff H-type section was performed by King at el. at the Boundary Layer Wind Tunnel Laboratory of the University of Western Ontario in Ontario, Canada (Kim 2007).

Fig. 1 shows the transfer functions in the lift direction. The proposed method yields relatively well-matched results to the measured transfer functions, which show more complicated variations. Although the RFA yields somewhat different results from the proposed method, the differences found other than in the $h\alpha$ component appear to be acceptable. However, the RFA yields completely inconsistent results for the $h\alpha$ component with the measured transfer function. In Fig. 1(b) and Fig. 1(d), the $h\alpha$ component evaluated by the RFA is drawn against the right vertical axis, which has a 20 times larger scale than the left axis. The real and imaginary parts of the $h\alpha$ component obtained by the RFA suddenly increase rapidly in an almost diverging fashion for the reduced frequency smaller than 1.0. This implies that the RFA yields unreliable results of a time-domain analysis for high wind velocities, which are of engineering importance in the design of a bridge.

Fig. 2 shows the impulse response functions obtained by the three approaches. It is clearly seen that the measured impulse response functions do not satisfy the causality condition. Especially, the causality of the $h\alpha$ component is severely violated. However, the proposed method restores the causality conditions for all of the regular components of the impulse response functions within the specified tolerance. The RFA results in very unstable impulse response functions, which increases rapidly as the dimensionless time approaches zero. The $h\alpha$ component of the impulse response function obtained by the RFA is drawn against the right vertical axis. The scale of the right vertical axis is 4 times larger than the left vertical axis. Unlike the other components, the RFA yields an increasing $h\alpha$ component with time in absolute sense, which is completely unreasonable from a physical point of view. As the impulse response function represents the influence of a unit motion on the aerodynamic forces at time t, the absolute value of the impulse response function should be a decreasing function with time.

5. CONCLUSION

A new approach is proposed for evaluating the impulse response functions required in the convolution integrals of aerodynamic forces acting on bridge decks. As the transfer functions formed by measured flutter derivatives generally violate the causality condition of the impulse response functions, an optimization scheme, in which the causality condition is imposed as a penalty function, is formulated in order to find the transfer functions closest to the measured ones. The transfer functions are interpolated with the cubic spline between two adjacent extraction points of the flutter derivatives. It is believed that the RFA has certain deficiencies in terms of determining the correct impulse response functions of bluff sections. Meanwhile, the cubic spline utilized in this study is able to fit a wide range of curves in a piecewise fashion with sufficient smoothness. Consequently, the proposed method can be applied to not only streamline sections with nearly monotonic transfer functions but also bluff sections with wiggling transfer functions.

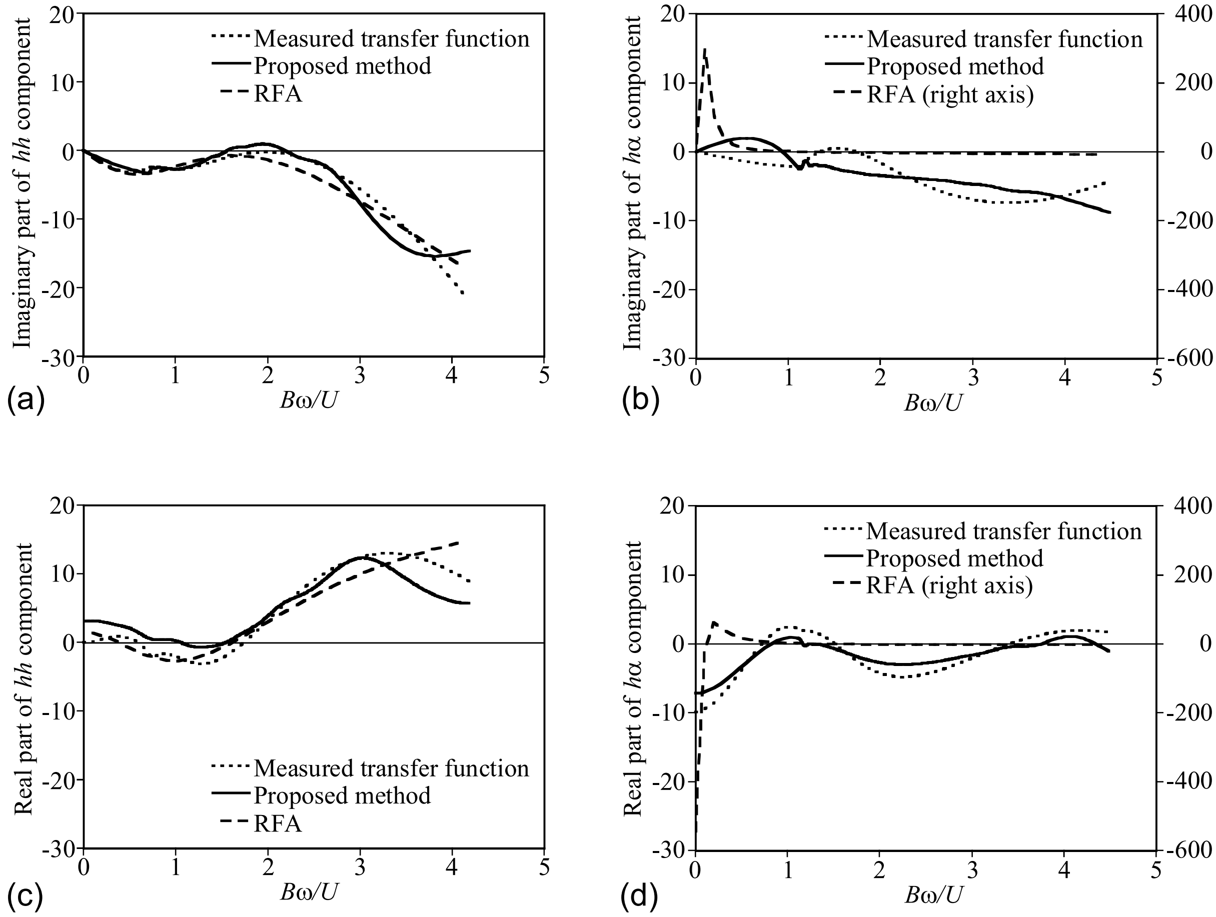

Fig. 1. Transfer functions of the bluff H-type section for the lift force: (a) imaginary part of the *hh* component, (b) imaginary part of the *h*α component, (c) real part of the *hh* component and (d) real part of the *h*α component (The *h*α component of RFA is drawn against the right vertical axis)

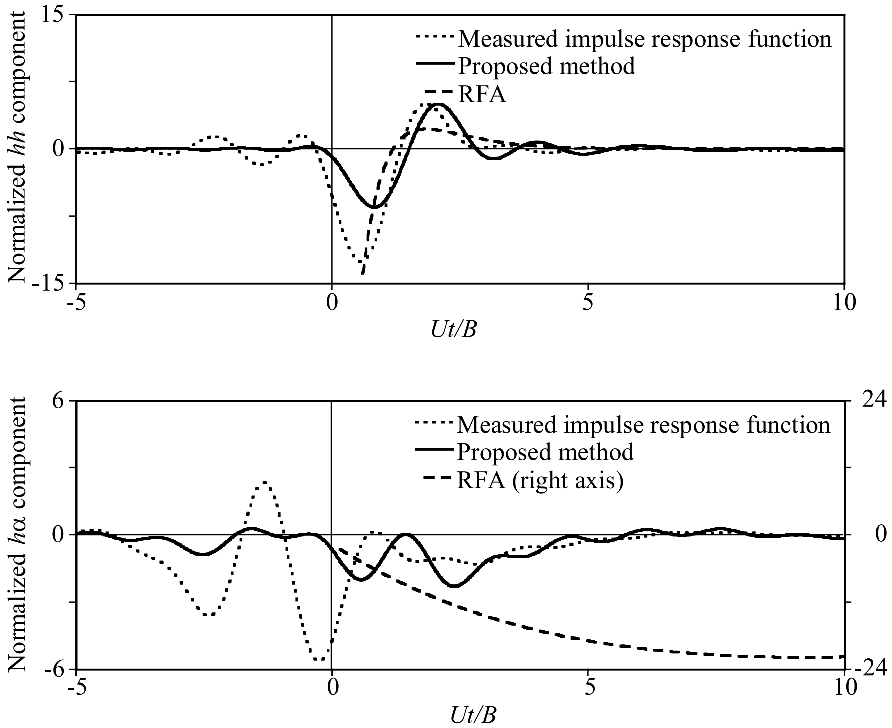

(a)

(b)

Fig. 2. Regular component of the normalized impulse response functions of the bluff H-type section: (a) *hh* component and (b) $h\alpha$ component (The $h\alpha$ component of RFA is drawn against the right vertical axis)

6. ACKNOWLEDGEMENT

This research was supported by the grant (09CCTI-A052531-05-000000) from the Ministry of Land, Transport and Maritime of Korean government through the Core Research Institute at Seoul National University for Core Engineering Technology Development of Super Long Span Bridge R&D Center.

REFERENCES

Caracoglia, L. and Jones, N.P. (2003). "Time domain vs. frequency domain characterization of aeroelastic forces for bridge deck sections", *J. Wind Eng. Ind. Aerodyn.,* Vol. **91**(3), 371-402.
Chen X., Matsumoto M. and Kareem A. (2000). "Time domain flutter and buffeting response analysis of bridges." *J. Eng. Mech.*, 126(1), 7–16.
Chen X. and Kareem A. (2003). "New frontiers in aerodynamic tailoring of long span bridges: an advenced analysis framework." *J. Wind. Eng. Ind. Aerodyn.*, 91(12-15), 1511–1528.

Jung, K., Kim, H.K. and Lee, H.S. (2012). “Evaluation of impulse response functions for convolution integrals of aerodynamic forces by optimization with a penalty function,” *J. Eng. Mech., ASCE,* 138(5), 519-529.
Katsuchi H., Jones N. P. and Scanlan R. H. (1999). “Multimode coupled flutter and buffeting analysis of the Akashi-Kaikyo Bridge.” *J. Struct. Eng*., 125(1), 60-70
Scanlan R. H. and Tomko J. J. (1971). “Airfoil and bridge deck flutter derivatives.” *J. Eng. Mech. Div.,* 97(6), 1717-1737.
Kim J. D. and King J. P. C. (2007). “The development of wind tunnel test technique for an aeroelastic buffeting analysis of long-span bridges.” BLWTL-SS19-2007-DRAFT report submitted to Korea Wind Engineering Research Center, the Boundary Layer Wind Tunnel Laboratory of the University of Western Ontario.